Stem Cell Reports
Article

ISSCR

OPEN ACCESS

Lysophosphatidic Acid Receptor Is a Functional Marker of Adult Hippocampal Precursor Cells

Tara L. Walker,[1] Rupert W. Overall,[1] Steffen Vogler,[2] Alex M. Sykes,[3] Susann Ruhwald,[1] Daniela Lasse,[2] Muhammad Ichwan,[1] Klaus Fabel,[1,2] and Gerd Kempermann[1,2,*]

[1]CRTD – Center for Regenerative Therapies Dresden, Technische Universität Dresden, Dresden 01307, Germany
[2]German Center for Neurodegenerative Diseases (DZNE) Dresden, Dresden 01307, Germany
[3]Max Planck Institute for Molecular Cell Biology and Genetics, Dresden 01307, Germany
*Correspondence: gerd.kempermann@crt-dresden.de
http://dx.doi.org/10.1016/j.stemcr.2016.03.002

SUMMARY

Here, we show that the lysophosphatidic acid receptor 1 (LPA_1) is expressed by a defined population of type 1 stem cells and type 2a precursor cells in the adult mouse dentate gyrus. LPA_1, in contrast to Nestin, also marks the quiescent stem cell population. Combining LPA_1-GFP with EGFR and prominin-1 expression, we have enabled the prospective separation of both proliferative and non-proliferative precursor cell populations. Transcriptional profiling of the isolated proliferative precursor cells suggested immune mechanisms and cytokine signaling as molecular regulators of adult hippocampal precursor cell proliferation. In addition to LPA_1 being a marker of this important stem cell population, we also show that the corresponding ligand LPA is directly involved in the regulation of adult hippocampal precursor cell proliferation and neurogenesis, an effect that can be attributed to LPA signaling via the AKT and MAPK pathways.

INTRODUCTION

Neurogenesis in the adult mouse hippocampus has by now been very well characterized; however, despite considerable effort, the identification and isolation of the underlying neural stem cells has been hampered by the lack of appropriate markers. Nestin is the most widely used marker of the stem cell population in the adult dentate gyrus and subventricular zone (SVZ). However, in Nestin-GFP transgenic mice the GFP expression is not restricted to the neural stem cells (Kawaguchi et al., 2001; Mignone et al., 2004). Nestin-GFP expression can also be found in immature neurons and when cultured in vitro as neurospheresf, only 0.4% of cells formed neurospheres (Mignone et al., 2004). SOX2 is another widely used stem cell marker, but its cell-type specificity is also not sufficient for many concerns. A large fraction of classical astrocytes ($S100\beta^+$), for example, expresses SOX2 (Couillard-Despres et al., 2006; Suh et al., 2007), with a recent study showing that approximately 30% of all SOX2-GFP^+ cells in the dentate gyrus are positive for S100β, a marker that is not expressed by the stem cells (Bracko et al., 2012). While several workable hippocampal stem cell isolation protocols have been proposed (Jhaveri et al., 2010; Walker et al., 2007, 2013), there is agreement in the field that there is still much room for further improvement.

Based on its expression pattern, we identified the lysophosphatidic acid receptor 1 (LPA_1)-GFP transgenic mouse as a potential tool for the isolation of adult hippocampal stem cells (Heintz, 2004). The importance of lipid metabolism in neural stem cell biology was highlighted with the identification of a direct function of lipid signaling in stem cell-based neural plasticity. The key enzyme for de novo lipidogenesis, fatty acid synthase (FASN), is not only active in neural stem cells, but its inhibition also impairs adult hippocampal neurogenesis (Knobloch et al., 2013). Among the potential lipid-based regulatory molecules, phospholipids are the primary candidates. Phospholipids are found in large amounts in the brain as the key components of the cellular lipid bilayer. Lysophosphatidic acid (LPA) is a membrane-synthesized phospholipid that acts as an intercellular signaling molecule through six G-protein receptor subtypes (LPA_{1-6}; Choi et al., 2010). The first of these receptors to be described, LPA_1, mediates the proliferation, migration, and survival of neural progenitor cells during development (Estivill-Torrus et al., 2008). There have also been reports that LPA_1 deletion reduces adult hippocampal neurogenesis (Matas-Rico et al., 2008) and causes spatial memory deficits (Castilla-Ortega et al., 2011; Santin et al., 2009). These findings suggested to us that LPA_1 might play a functional role in adult hippocampal neurogenesis. In addition, the nature of LPA_1 as a surface receptor made it a potential candidate for the prospective isolation of hippocampal precursor cells.

Given the possible functional links between LPA_1 and adult neurogenesis, we undertook the present study to determine whether the receptor LPA_1 might indeed serve as a marker for the identification and prospective isolation of adult hippocampal stem cells and whether its ligand, the phospholipid LPA, might exert specific pro-neurogenic effects.

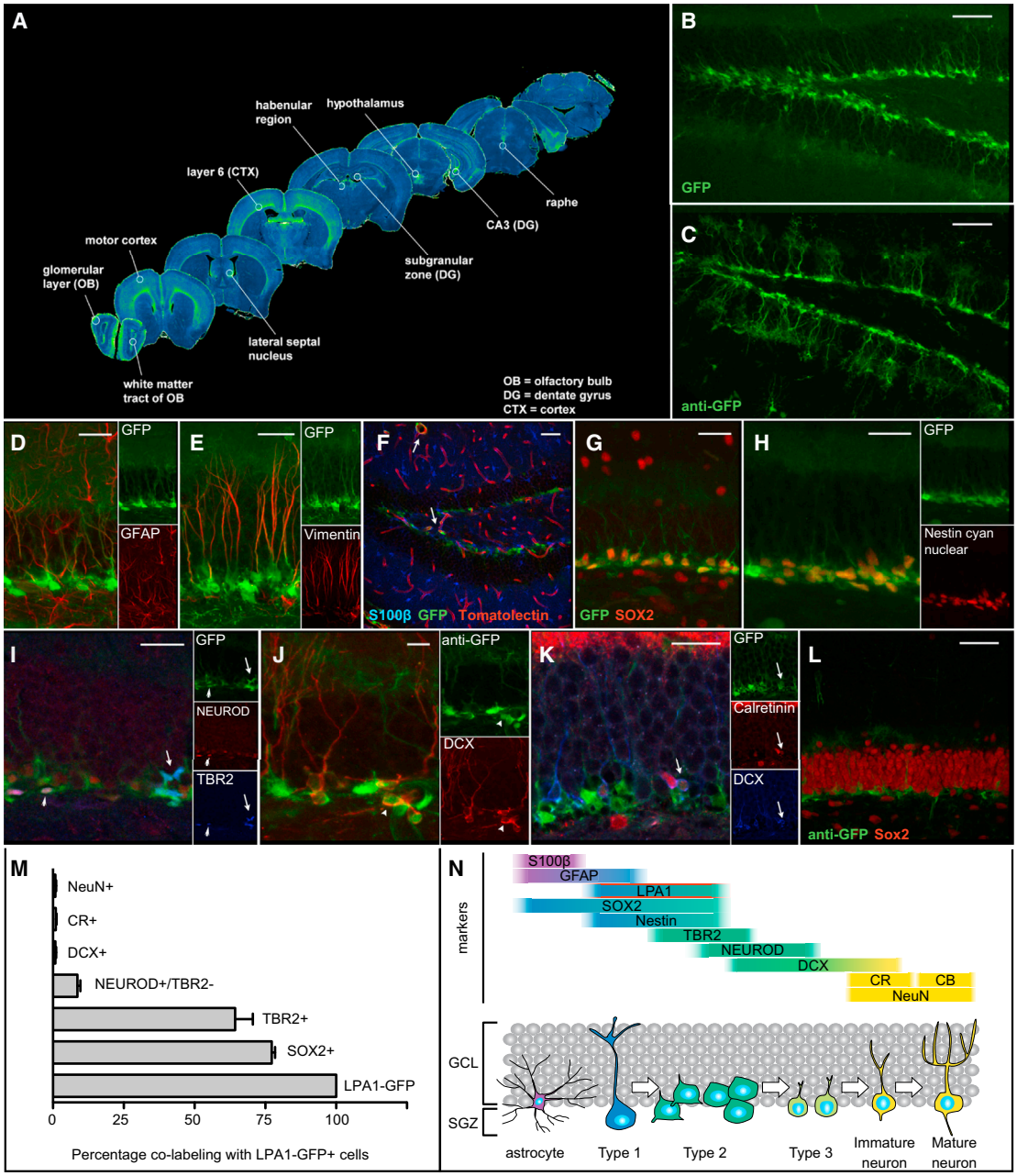

Figure 1. LPA_1-GFP Is Expressed in the Precursor Cells of the Adult Dentate Gyrus

(A–E) GFP^+ cells in the adult brain are detected in various brain regions (A) including the adult dentate gyrus (B). The GFP signal in the dentate gyrus resembles that in the Nestin-GFP mouse (C); however, the processes of the radial-glia-like stem cells show less prominent GFP immunofluorescence (D). The processes of some LPA_1-GFP^+ cells (green) co-express GFAP (red) and vimentin (red, E).

(F–L) We could not detect co-localization of LPA_1-GFP with S-100β (F, blue) in the dentate gyrus. LPA_1-GFP rarely co-localized with tomato lectin-stained blood vessels (F, red, arrows). Abundant co-localization of SOX2 (red) and GFP (green) is observed (G). (H) Linear unmixing of LPA_1-GFP (green) and Nestin-cyan nuclear (red) shows almost complete overlap in the progenitors in the SGZ. (I) GFP^+ cells in the dentate gyrus express TBR2 (blue, arrow) and several cells express GFP, TBR2, and NeuroD (red, arrowhead). Very few cells are DCX^+ and GFP^+ (J [red, arrowheads] and K [blue, arrow]). In general, GFP^+ cells (G, green) do not express NeuN (L, red) or calretinin (K, red). Double-positive cells were very rarely found (K).

(legend continued on next page)

RESULTS

LPA_1 Is Expressed by Radial-Glia-like Precursor Cells of the Adult Dentate Gyrus but Shows Limited Expression in the SVZ

Using the LPA_1-GFP reporter mouse line (Gong et al., 2003), we first mapped LPA_1-GFP expression along the entire ventral-dorsal axis of the adult brain (Figures 1A and S1). LPA_1-GFP expression was detected in the subgranular zone (SGZ) of the dentate gyrus (Figure 1B) and very closely resembled the characteristic Nestin-GFP signal (Figure 1; Yamaguchi et al., 2000). Glial fibrillary acidic protein (GFAP) immunofluorescence revealed co-localization in the processes of $GFAP^+$ and LPA_1-GFP^+ cells in the SGZ (Figure 1D), indicating that they are radial-glia-like type 1 cells (Kempermann et al., 2004). This was confirmed by staining for another astrocytic marker, vimentin (Figure 1E). No co-localization of LPA_1-GFP^+ was detected with S100β, a marker of post-mitotic astrocytes in the murine hippocampus (Figure 1F). As expected, there was significant overlap in expression between LPA_1 and the precursor marker Sox2 (77.25% ± 1.2%; Figure 1G). Crossing LPA_1-GFP mice with nuclear Nestin-Cyan mice (Encinas and Enikolopov, 2008) revealed that almost all GFP^+ cells were also $Cyan^+$ (Figure 1H). The majority of LPA_1-GFP^+ cells were early progenitors (LPA_1-GFP^+Tbr2^+: 64.5% ± 6.3%; Figure 1; Hodge et al., 2008). LPA_1-GFP^+ expression also identified a fraction of type 2b cells (LPA_1-$GFP^+NeuroD^+Tbr2^-$: 4.3% ± 0.1%). Only very few LPA_1-GFP^+ cells co-expressed doublecortin (DCX) (0.9% ± 0.2%; Figures 1J and 1K) or NeuN (0.9% ± 0.2%; Figure 1L) and calretinin (0.1% ± 0.1%; Figure 1K). Outside the dentate gyrus, LPA_1-GFP^+ expression was not restricted to precursor cells (Figure S2). These data indicate that LPA_1 in the dentate gyrus is a specific marker of type 1 stem cells and early progenitor cells.

LPA_1-GFP Mice Can Be Used to Directly Quantify the Exercise-Induced Increase in Precursor Proliferation

To determine whether LPA_1-GFP mice could be used to directly detect in vivo changes in precursor cell numbers, we used the physical activity paradigm (van Praag et al., 1999). Quantification of bromodeoxyuridine (BrdU)-labeled cells revealed the expected increase in proliferation following physical activity (standard housing 2,977 ± 162.8 $BrdU^+$ cells, n = 11 mice versus running 4,869 ± 475.8 $BrdU^+$ cells, n = 12 mice, p = 0.0016; Figures 2B and 2C). Similarly this could be directly quantified by counting LPA_1-GFP^+ cells (standard housing 7,176 ± 512 LPA_1-GFP^+ cells, n = 11 mice versus running 10,220 ± 562.9 LPA_1-GFP^+ cells, n = 12 mice, p = 0.0007; Figures 2D and 2E). The running-induced increase in proliferation could also be directly detected by flow cytometric quantification of LPA_1-GFP^+ cells (Figures 2F–2H: standard housing 14.2% ± 0.7%, n = 4 mice versus running 20.4% ± 1.7%, n = 4 mice, p = 0.0142), thus confirming that LPA_1-GFP mice are a useful tool to directly detect in vivo changes in hippocampal precursor proliferation.

Sorting LPA_1-GFP^+ Cells Allows the Prospective Isolation of Hippocampal Precursor Cells

Given that we could detect LPA_1-GFP expression in the precursor cells of the adult DG by immunofluorescence, we next examined whether we could prospectively isolate hippocampal precursor cells on the basis of LPA_1-GFP expression. Firstly, the baseline precursor frequency of unfractionated cells, gating only on forward and side scatter and propidium iodide (live cells), was determined (2.4 ± 1.3 neurospheres per 1,000 total cells). Sorting on the basis of LPA_1-GFP expression enhanced the frequency of precursor cells to 19.9 ± 5.5 neurospheres per 1,000 cells, and neurospheres formed almost exclusively from the LPA_1-GFP^+ population (LPA_1-GFP^+ 99.8% ± 0.2% versus LPA_1-GFP^- 0.2% ± 0.2% of total neurospheres, n = 4 experiments; p = 0.0001; Figures 3A–3D). Plating the LPA_1-GFP^+ population in the presence of depolarizing levels of KCl, which we have previously shown activates a latent stem cell population (Walker et al., 2008), increased the number of neurospheres (LPA_1-GFP^+, no KCl 19.9 ± 5.5 versus KCl 24.4 ± 6.4 neurospheres per 1,000 cells, n = 4 experiments, p = 0.03) but had no effect on the LPA_1-GFP^- cells (LPA_1-GFP^- no KCl 0.03 ± 0.03 versus KCl 0.02 ± 0.02 neurospheres per 1,000 cells, n = 4 experiments, p = 0.9).

Given that Nestin is a commonly used marker of neural precursor cells, we next compared the efficacy of precursor isolation using the LPA_1-GFP transgenic mice with that of Nestin-GFP mice. Although the majority of the neurospheres were formed from the Nestin-GFP^+ population (Nestin-GFP^+ 33.8 ± 6.1 versus Nestin-GFP^- 2.0 ± 0.4 neurospheres per 1,000 cells, n = 6 experiments, p = 0.0022; Figure 3D), a large percentage of the total neurosphere formation was from the Nestin-GFP^- cells (Nestin-GFP^+ 73.5% ± 9.6% versus Nestin-GFP^- 26.5% ± 9.6%). In

(M) A summary plot of the fraction of LPA_1-GFP^+ cells that co-localize with other markers (n = 4 individual mice with a total of 800 cells for each antibody combination).

(N) Schematic illustration of expression of individual markers in relation to LPA_1-GFP expression.

Scale bars represent 50 μm in (B), (C), (F), and (L) and 25 μm in all other panels. (A) is a compilation of images of coronal sections, (I) and (K) are single planes of z stacks, and the other panels are maximum-intensity projections of z stacks.

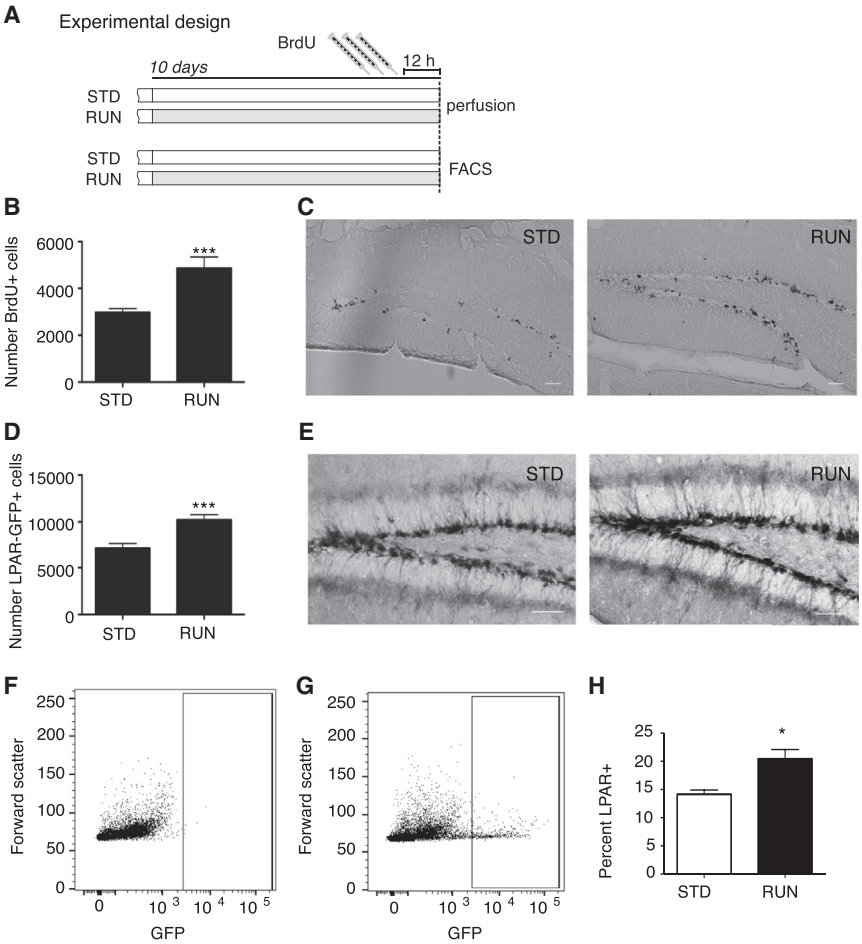

Figure 2. A Running-Induced Increase in Proliferation Can Be Measured Directly in LPA_1-GFP Mice

(A and B) Experimental design (A) and histogram (B) representing the number of BrdU-labeled cells in running (RUN) and standardly housed (STD) LPA_1-GFP mice. n = 11 mice per group, ***p < 0.001, Student's t test.

(C) Representative images of BrdU labeling in the dentate gyrus. Scale bars represent 50 μm.

(D) Histogram representing the number of LPA_1-GFP^+ cells in RUN and STD housed LPA_1-GFP mice. n = 11 mice per group, ***p < 0.001, Student's t test.

(E) Representative image of LPA_1-GFP labeling in the dentate gyrus. Scale bars represent 50 μm.

(F–H) FACS plot of a wild-type littermate used to set the GFP gates (F). LPA_1-GFP^+ cells were analyzed from RUN (G) or STD housed mice with the gates set to count total GFP^+ cells. Histograms representing the percentage of total LPA_1-GFP^+ cells (H, n = 4 mice per group, *p < 0.05, student's t-test) in RUN or STD mice.

All data represent the mean ± SEM.

contrast to the LPA_1-GFP^- population, the Nestin-GFP^- population contained a population of latent stem cells that could be activated by depolarizing levels of KCl (Nestin-GFP^+, no KCl 30.32 ± 5.9 versus KCl 27.9 ± 4.0, p = 0.9 versus Nestin-GFP^-, no KCl 2.0 ± 0.2 versus KCl 2.5 ± 0.2 neurospheres per 1,000 cells, n = 6 experiments, p = 0.04). Therefore, compared with Nestin-GFP, LPA_1-GFP can be used to isolate both the active and quiescent precursor cells from the adult dentate gyrus.

LPA_1-GFP^+ Precursor Cells Show Stem Cell Properties

In agreement with the results generated from the neurosphere assays, cells grown as adherent monolayers showed proliferation only from the LPA_1-GFP^+ cultures (Figures 3E and 3F). After four passages under proliferative conditions, >95% of cells were positive for Nestin and LPA_1-GFP (Figure 3G). Following differentiation, all three neural cell types (neurons, astrocytes, and oligodendrocytes) were generated from LPA_1-GFP^+ primary neurospheres (Figures 3H–3J), supporting multipotency. The majority of the cells were astrocytes (91.2% ± 1.3%), a small number were neurons (6.0% ± 1.3%), and few oligodendrocytes (1.1% ± 0.3%) were generated (n = 4 experiments). To examine self-renewal, we dissociated individual large (>200 μm) primary neurospheres, which we have previously shown to be stem cell derived (Walker et al., 2008), into single cells, replated them into neurosphere medium, and cultured them as individual cell lines. Approximately 20% of the primary neurospheres could be maintained over five passages (11 of 56 neurospheres), indicating their ability to self-renew. In addition, the adherent monolayer cultures generated both $GFAP^+$ astrocytes and βIII-$tubulin^+$ neurons following differentiation. Taken together, these results support the idea that the LPA_1-GFP-expressing cells from the dentate gyrus include multipotent, self-renewing stem cells.

LPA_1-GFP in Combination with EGF-Receptor and Prominin-1 Expression Effectively Separates the Proliferative from the Non-proliferative Precursor Cells

The LPA_1-GFP^+ population was relatively large and had a neurosphere-forming frequency of approximately 1 in 50

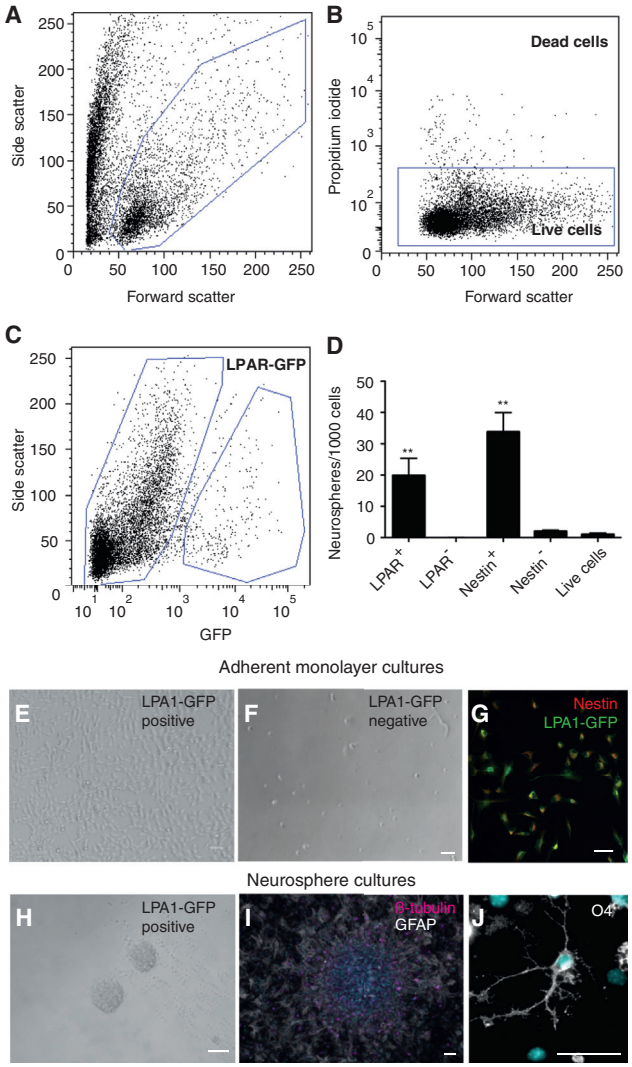

Figure 3. LPA_1-GFP^+ Precursor Cells Can Be Prospectively Isolated from the Adult Dentate Gyrus and Are Multipotent In Vitro

(A–C) Cells isolated from the dentate gyrus of LPA_1-GFP^+ mice are first gated on the basis of forward and side scatter (A) and excluding dead cells (B). Approximately 5% of cells in the adult dentate gyrus are LPA_1-GFP^+ (C).

(D) Histogram representing the number of neurospheres generated per 1,000 cells for each isolated population. $F_9 = 13.3$, $^{**}p < 0.01$, one-way ANOVA with Tukey's multiple comparison test, n = 4 experiments.

(E–J) LPA_1-GFP^+ and LPA_1-GFP^- cells were sorted and cultured independently as adherent monolayer cultures (E–G) or neurospheres (H–J). Cell proliferation was observed only from the LPA_1-GFP^+ cultures (E), with no growth from the LPA_1-GFP^- cells (F). After five passages under proliferative conditions, the majority of the cells remained positive for the precursor markers LPA_1-GFP (green) and Nestin (red) (G). The primary neurospheres generated from the LPA_1-GFP^+ cells (H) can differentiate into βIII-tubulin$^+$ (I, magenta) neurons, $GFAP^+$ astrocytes (I, white), and $O4^+$ oligodendrocytes (white, J). $DAPI^+$ cell nuclei are cyan (I, J).

Data represent the mean ± SEM. Scale bars, 50 μm.

cells. This was increased to approximately 1 in 7 by isolating cells with high levels of LPA_1-GFP expression (LPA_1-GFP^{high} 135.5 ± 30.5 versus LPA_1-GFP^{low} 13.7 ± 2.3 neurospheres per 1,000 cells, n = 3 experiments, p = 0.05; Figure S3A). Activated stem cells and proliferative progenitor cells can also be isolated from the adult SVZ (Pastrana et al., 2009) and dentate gyrus (Walker et al., 2013) on the basis of epidermal growth factor receptor (EGFR) expression. As expected, the LPA_1-GFP^+EGFR^+ population contained most of the proliferative cells (205.2 ± 32.8 neurospheres per 1,000 cells) compared with the LPA_1-GFP^+EGFR^- (4.5 ± 0.02 neurospheres per 1,000 cells), the LPA_1-GFP^-EGFR^+ (2.8 ± 0.05 neurospheres per 1,000 cells), and the LPA_1-GFP^-EGFR^- (0.1 ± 0.03 neurospheres per 1,000 cells; n = 3 experiments, p = 0.0021; Figure S3B) populations. The neurosphere-forming frequency of the LPA_1-GFP^+EGFR^+ population increased to 1 in 4.9 cells.

Finally, we have previously shown that adult hippocampal stem cells express prominin-1 (Walker et al., 2013). A combination of all three markers (LPA_1-GFP, EGFR, and prominin-1) increased the purity of the proliferative population to one neurosphere formed per 3.2 cells plated (LPA_1-GFP^+EGFR^+prominin-1^+ 310.6 ± 31.7, LPA_1-GFP^+EGFR^-prominin-1^+ 13.3 ± 4.9; LPA_1-GFP^+EGFR^+ prominin-1^- 102.0 ± 39.8 neurospheres per 1,000 cells, n = 3 experiments, p = 0.001; Figure S3C). The expected theoretical maximum frequency of acutely counted, potential neurosphere-forming cells that survive the sorting procedure has been estimated to be between 1 in 2 (our observations) and 1 in 6 (Kawaguchi et al., 2001). The above combination of markers therefore allows us to isolate an essentially pure population of proliferating neurosphere-forming cells.

Proliferative Precursor Cells from the Adult Dentate Gyrus Have a Distinct Transcriptional Profile

Using the combination of LPA_1-GFP, prominin-1, and EGF-647, we are able to separate the highly proliferative (i.e., neurosphere-forming) LPA_1^+ cells from the non-proliferative population. To gain insight into the underlying molecular regulation of these distinct subpopulations of LPA_1^+ cells, we performed RNA sequencing on three fluorescence-activated cell sorting (FACS)-isolated primary cell populations; "proliferative LPA_1^+ cells" (LPA_1-GFP^+EGFR^+prominin-1^+), "non-proliferative LPA_1^+ cells" (LPA_1-GFP^+EGFR^+prominin-1^-, LPA_1-GFP^+EGF^-prominin-1^+, and LPA_1-GFP^+EGFR^-prominin-1^-), and "niche cells" (LPA_1-GFP^-), a heterogeneous population that is composed predominantly of neurons ($NeuN^+$: 46.8% ± 2.7%, n = 4 experiments; Figures 4A–4C).

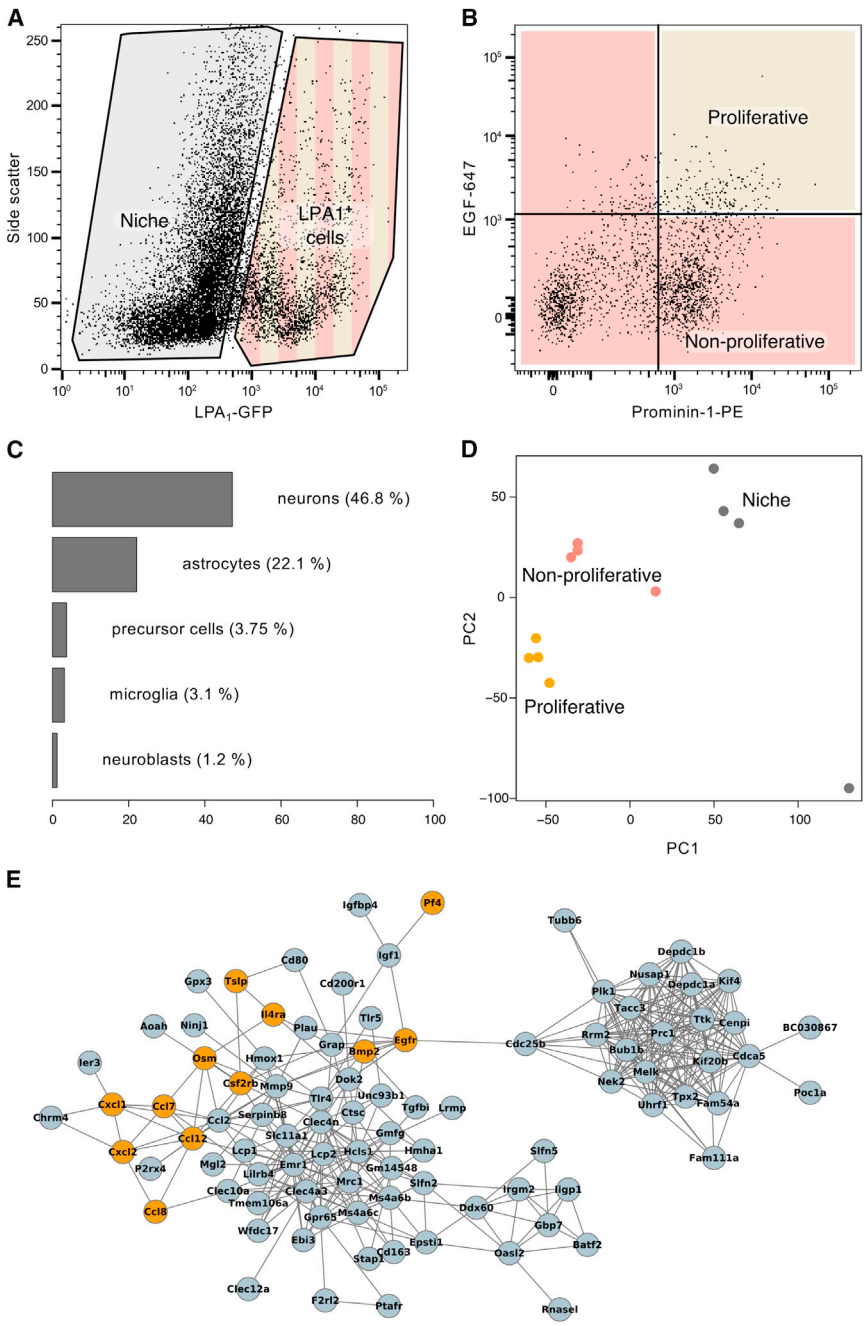

Figure 4. RNA Sequencing of the Proliferative Precursor Population Reveals Enrichment in Immune-Response-Associated Genes

(A–E) Dissociated dentate gyrus was sorted into LPA_1-GFP$^-$ (non-precursor "niche" cells) and LPA_1-GFP$^+$ (precursor cells) populations (A), and a subset of the precursors were further enriched for proliferative cells based on EGFR and prominin-1 expression, with the remainder being classed as non-proliferative precursor cells (B, n = 4 independent experiments). The LPA_1-GFP$^-$ population was a mixture of other cell types, predominantly neurons, comprising the niche (C). A principal component analysis showed samples to cluster by cell population (D). A pathway enrichment analysis of the proliferative population using the KEGG database revealed a significant association with "cytokine-cytokine receptor interaction," and genes from this pathway (orange nodes) cluster together when highlighted on a STRING interaction network (E). The STRING network was generated using the list of proliferative cell genes, but genes with no connections were not drawn.

A principal component analysis showed that, as expected, the samples cluster by cell population (Figure 4D). We identified a set of 255 genes expressed only in the precursor cells (all LPA_1^+ cells compared with LPA_1^- cells) and a subset of 145 genes with specific expression only in the proliferative neurosphere-forming cells (LPA_1-GFP$^+$EGFR$^+$prominin-1$^+$; Tables S1 and S2). As expected, the combined precursor population was enriched in the gene ontology (GO) categories of "cell division" (GO:0051301, $p = 3.9 \times 10^{-15}$) and "cell cycle" (GO:0007049, $p = 3.9 \times 10^{-15}$), confirming its highly proliferative nature (Table S3). A GO analysis of the proliferative LPA_1^+ cells revealed a unique functional profile, with an enrichment in terms related to the immune response such as "immune system process" (GO:0002376, $p = 1.6 \times 10^{-10}$), "immune response" (GO:0006955, $p = 4 \times 10^{-9}$), and "inflammatory response" (GO:0006954, $p = 5.3 \times 10^{-7}$; Table S4). A survey of the KEGG database revealed that our set of proliferative precursor cell genes was enriched in the pathways "cytokine-cytokine receptor interaction" ($p = 1.3 \times 10^{-5}$) and "chemokine signaling pathway"

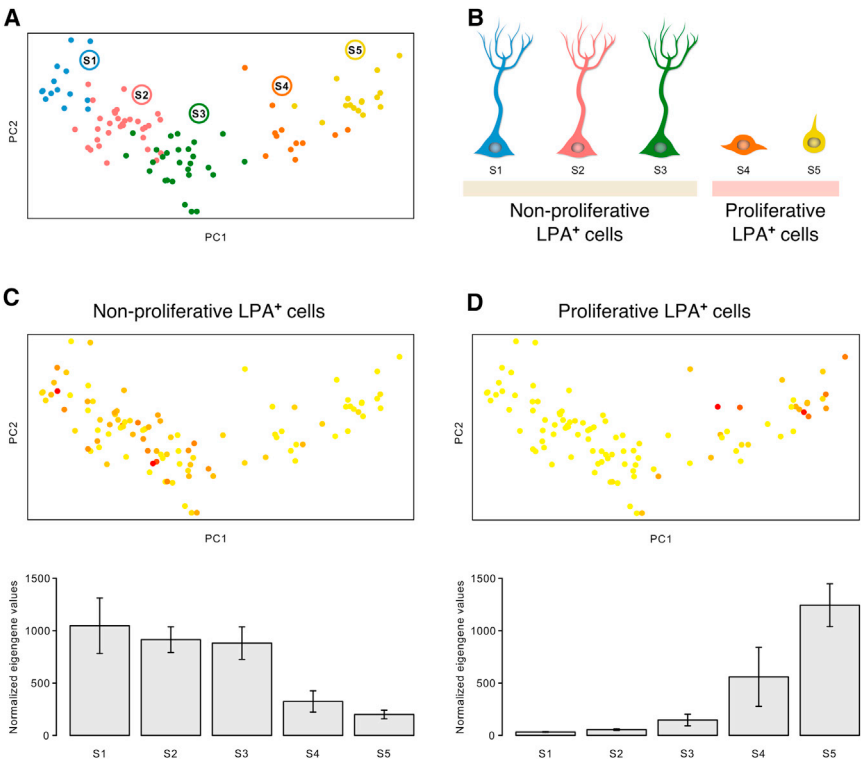

Figure 5. The Two LPA_1-GFP$^+$ Populations Correspond to Subpopulations Proposed by Existing Single-Cell Sequencing Data

(A) Clustering of single cells identified by principal component analysis of RNA-sequencing data from Shin et al. (2015) (figure adapted from original manuscript).

(B) The five subpopulations (S1–S5) correspond to the proliferative and non-proliferative LPA_1^+ populations identified in the current study.

(C and D) Normalized eigengene expression profiles in the Shin et al. dataset for the genes we found enriched in non-proliferative (C) and proliferative (D) LPA_1^+ cells are plotted on the clustering graph (upper panels) and as mean ± SD for each subpopulation (lower panels; n = 4 experiments).

($p = 3 \times 10^{-3}$). Interestingly, when viewed as a STRING protein-protein interaction network (Franceschini et al., 2013), many of the KEGG pathway-enriched genes clustered together, further suggesting that they are functionally similar (Figure 4E). This same network also contains a tight cluster of genes involved in cell division. Given that these GO and KEGG profiles are also characteristic of circulating immune cells, we had to exclude potential contamination with blood cells. Using flow cytometry, we confirmed that our proliferative cell population did not contain any lymphocytes ($CD45^+$) or endothelial cells ($CD31^+$; Figure S4). Together these results show that, while the total precursor cell population exhibited the expected mitotic phenotype, the highly proliferative neurosphere-forming population is distinguished by an unexpected transcription profile, suggesting a role for cytokine signaling in these cells.

A recent study further differentiated hippocampal Nestin-positive cells into five subpopulations (S1–S5) based on their molecular profiles, with characteristics ranging from quiescent stem cells to actively dividing precursors (Shin et al., 2015) (Figures 5A and 5B). Comparison of the expression profiles of our proliferative and non-proliferative precursor cells with the expression data from that study showed that our non-proliferative cells exhibited a profile similar to that of the S1–S3 stages, identified by Shin et al. (2015) as the non-dividing putative stem cell subpopulations (Figure 5C), whereas our proliferative population corresponded to the actively dividing S4 and S5 stages (Figure 5D).

CXCL1 Increases Hippocampal Neurosphere Number

As a case study to investigate the role of immune-associated genes in adult hippocampal precursor proliferation, we chose three cytokines that were highly expressed in our stem cell population, CXCL1, CXCL2, and CCL8. Whether these three cytokines play a role in neural precursor cell proliferation was unknown. CXCL2 and CCL8 had no effect on the size or number of neurospheres generated from either SVZ or dentate gyrus primary cells (Figure S5). CXCL1, however, significantly increased the number of neurospheres generated from both the SVZ (30 ng/ml CXCL1 137.1% ± 6.2% of control, p = 0.009, n = 4 experiments) and the dentate gyrus (3 ng/ml CXCL1 173.0% ± 10.8% of control, p = 0.02, n = 3 experiments; Figure S5). This exemplary result confirms the regulatory role of one of the identified immune-related cytokines in adult hippocampal precursor proliferation.

LPA Increases Hippocampal Precursor Proliferation In Vitro

In combination, the data presented above suggest that LPA_1-GFP is expressed with high specificity on type 1 and type 2a hippocampal precursor cells in vivo. However, the direct effect of LPA on the proliferation and survival

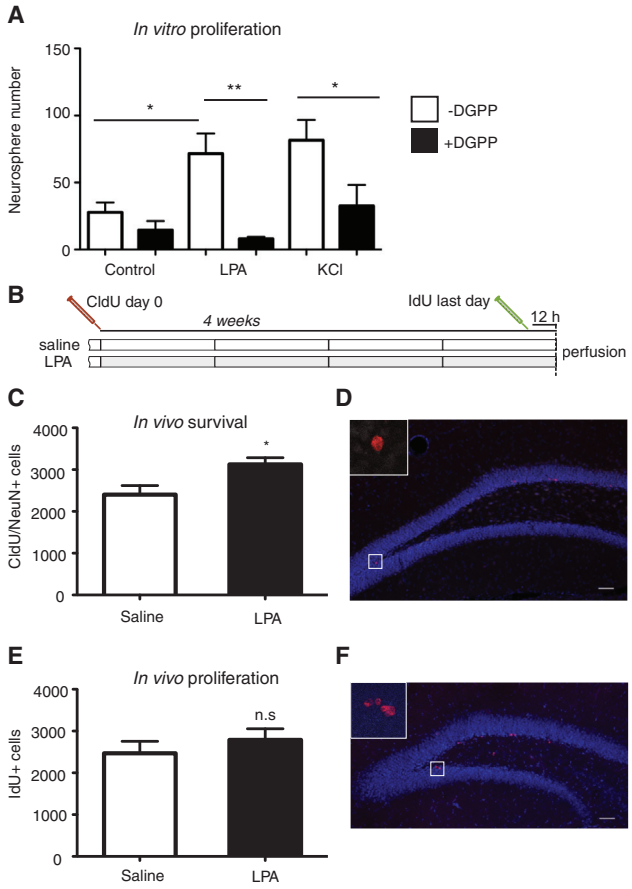

Figure 6. LPA Increases Precursor Proliferation In Vitro and In Vivo

(A) Histogram representing the number of neurospheres formed from primary adult dentate gyrus cells treated with 10 μM LPA or 15 mM KCl in the presence or absence of the LPA inhibitor DGPP. F_{23} = 8.3, *p < 0.05, **p < 0.01, one-way ANOVA with Tukey's multiple comparison test, n = 4 experiments.

(B) Experimental design for in vivo LPA infusion and thymidine analog labeling.

(C–F) Histograms representing the number of surviving neurons (C) and the number of proliferating precursor cells (E) following 28 days of LPA infusion. Two-tailed Student's t test, *p < 0.05, n = 11 animals (control group) and n = 12 animals (LPA group). Representative images of CldU (red) and NeuN (white) double-labeled cells (D) and IdU (red) single-labeled cells (F), DAPI-labeled nuclei (blue).

Data represent the mean ± SEM. Scale bars, 50 μm.

of these cells has not yet been examined. To investigate this, we first added LPA (10 μM) to cultured primary hippocampal precursor cells. Exogenous LPA significantly increased the number of neurospheres, as did the addition of depolarizing levels of KCl, a response that could be blocked by the specific LPA_1/LPA_3 antagonist diacylglycerol pyrophosphate (DGPP) (control 27.75 ± 7.39, LPA 71.50 ± 15.06, LPA + DGPP 8.00 ± 1.58, KCl 81.5 ± 15.2, KCl + DGPP 32.5 ± 15.8, n = 4 experiments, p = 0.0006; Figure 6A). LPA treatment also increased neurosphere size (control 51.5 ± 1.5 μm, LPA 69.3 ± 3.3 μm, n = 3 experiments, p = 0.04) but had no effect on the percentage of neurons (control 8.6% ± 2.3% versus LPA 11.5% ± 5.2%, p = 0.57, n > 8 coverslips) or astrocytes (control 82.1% ± 7.3% versus LPA 87.0% ± 4.8%, p = 0.62, n > 8 coverslips) after differentiation.

LPA Increases Net Neurogenesis without Changing Proliferation In Vivo

To confirm that the effect of LPA on hippocampal precursor cells in vivo, we used osmotic minipumps to continuously infuse LPA directly into the hippocampus for 28 days. To measure neuronal survival, we injected 5-chloro-2′-deoxyuridine (CldU) at the beginning of the experiment, and to label proliferating cells 5-iodo-2′-deoxyuridine (IdU) was injected 12 hr prior to perfusion (Figure 6B). We found an increase in neuronal survival ($CldU^+NeuN^+$ cells; saline 2,402 ± 215.1, n = 11 animals versus LPA 3,125 ± 161.6, n = 12 animals, p = 0.01; Figures 6C and 6D), indicating a significant effect of LPA on adult hippocampal neurogenesis. Interestingly, this effect did not appear to be due to a pro-proliferative effect, as we saw only a small but non-significant increase in proliferating (IdU^+) precursor cells in the 28-day LPA-infused group (saline 2,469 ± 286.4, n = 10 animals versus LPA 2,732 ± 266.5, n = 12 animals, p = 0.42; Figures 6E and 6F). Similarly, we also observed no significant increase in IdU^+ cells following 7 days of LPA infusion (saline 2,553 ± 302.9, n = 6 animals versus 2,656 ± 140.0, n = 7 animals, p = 0.8). These data show a specific effect of LPA on survival of newborn neurons.

LPA Signals through the AKT and the MAPK Pathways In Vitro and Ex Vivo

LPA can signal through several G-protein-coupled receptors ($LPA_{1–6}$) and multiple signaling pathways including AKT, mitogen-activated protein kinase (MAPK), or protein kinase C (PKC) to induce cell proliferation, differentiation, or survival of many cell types (Ye et al., 2002). We first performed a time-course experiment with LPA stimulations of between 2 and 60 min (Figure 7A). In these experiments, we found that LPA stimulation of adherent neural precursor cells in vitro rapidly and transiently induced phosphorylation of AKT (S473) 2 min after stimulation (ratio pAKT/AKT unstimulated 0.52 ± 0.02 versus 2 min 0.66 ± 0.09, n = 4 experiments, p = 0.02; Figure 7B) and ERK1/2 (ratio pERK/ERK unstimulated 0.23 ± 0.04, 2 min 1.41 ± 0.23, p = 0.0025, 5 min 1.47 ± 0.24, p = 0.0025, 10 min 0.83 ± 0.08, p = 0.0006; Figure 7C), an effect that was reduced to basal levels at 5 min (for AKT) and 30 min (for ERK1/2) after LPA administration. A similar effect was observed following

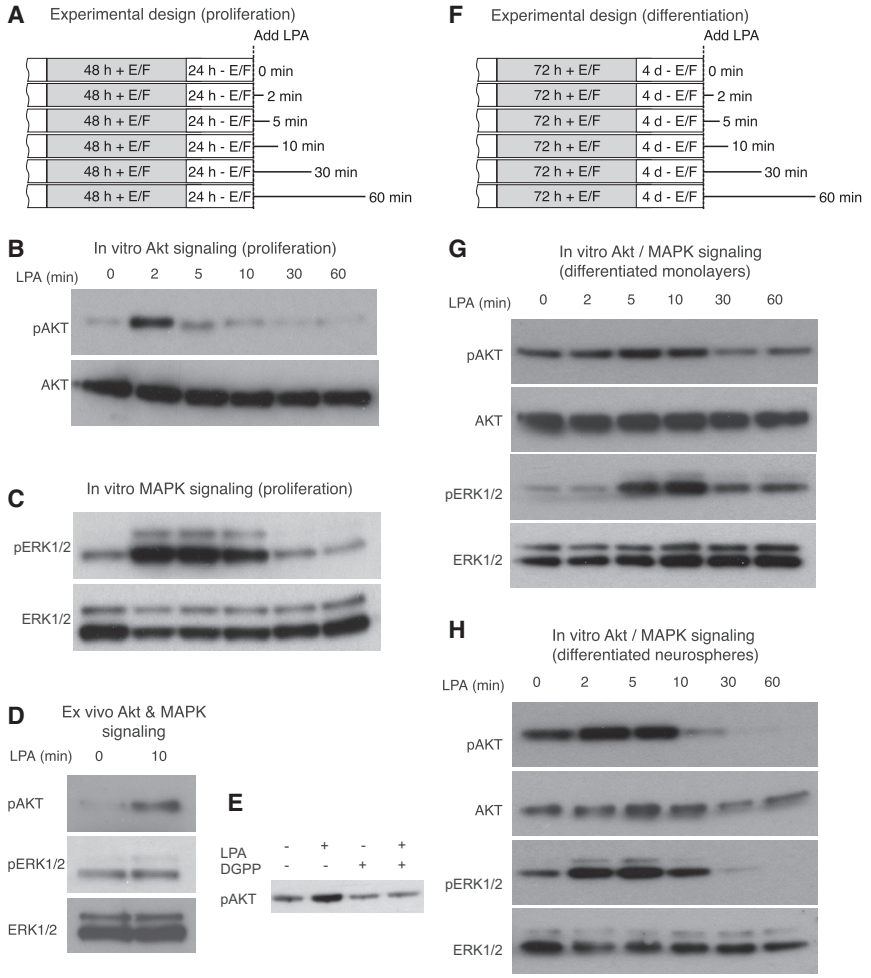

Figure 7. LPA Signals via the AKT and MAPK Pathways In Vitro

(A) Experimental design for in vitro LPA signaling under proliferation conditions.

(B–D) There is a rapid phosphorylation of AKT (B) and MAPK (C) in response to LPA treatment of adherent neural precursor cells in vitro and primary dentate gyrus cells in vivo (D, n = 4 experiments).

(E) The activation of AKT signaling can be blocked by the specific $LPA_{1/3}$ antagonist DGPP.

(F) Experimental design for in vitro LPA signaling under proliferation conditions.

(G and H) There is a rapid phosphorylation of AKT and MAPK in response to LPA treatment in both differentiated adherent monolayers (G) and differentiated neurospheres (H, n = 3 experiments).

10 min of LPA stimulation of primary isolated dentate gyrus cells ex vivo (Figure 7D). We confirmed that this signaling was occurring via the $LPA_{1/3}$ receptor as AKT phosphorylation was inhibited when the cells were pre-treated with the $LPA_{1/3}$-specific antagonist DGPP for 1 hr prior to the addition of LPA (Figure 7E). In addition, we confirmed that phosphorylation of AKT and MAPK in response to LPA stimulation also occurs in differentiated cells generated from both adherent monolayers (Figures 7F and 7G) and neurospheres (Figure 7H). These results demonstrate that LPA signals via the AKT and MAPK pathways, providing a functional context for this marker.

DISCUSSION

In the present study we show that LPA_1 is expressed by stem and progenitor cells (predominantly type 1 and type 2a) within the neurogenic niche of the dentate gyrus of adult mice, and that it outperforms Nestin, the current gold standard, as a marker for prospective isolation of cells that exhibit precursor cell properties ex vivo. Sorting LPA_1-GFP^+ cells in combination with prominin-1 and EGFR allows the separation of the non-proliferative from the proliferative precursor cells, the latter of which was revealed by RNA sequencing to have an unexpected immune-cell-like transcriptional profile.

The intermediate filament Nestin is the most commonly used marker of neural stem cells. Although all four commonly accessible transgenic Nestin-GFP lines show expression in the adult neurogenic regions, they differ in the extent of GFP expression (Beech et al., 2004; Kawaguchi et al., 2001; Mignone et al., 2004; Yamaguchi et al., 2000). It was recently demonstrated that Nestin expression is absent from the quiescent stem cell population of the adult SVZ (Codega et al., 2014), being upregulated only after the stem cells are activated. In the present study, we demonstrate that LPA_1-GFP is a more sensitive marker than Nestin-GFP and can be used to effectively isolate the proliferative hippocampal precursor population, with >99% of

the neurospheres generated from the LPA_1-GFP^+ cells. Importantly, LPA_1-GFP appears to also mark the quiescent stem cell population in the dentate gyrus. In contrast to the Nestin-GFP^- population, no quiescent stem cells could be activated from the LPA_1-GFP^- population following in vitro depolarization, a treatment which we have previously shown to mimic neural activity (Walker et al., 2008). Combining LPA_1-GFP expression with two other markers, EGFR and prominin-1, we were able to further separate the proliferative (neurosphere-forming) from the non-proliferative cells.

Our flow cytometric isolation strategy has allowed the molecular characterization of proliferative, as distinct from the non-proliferative precursor cells. This distinction could previously not be made using broader markers such as Nestin and SOX2. Indeed, comparison of our list of 145 proliferative precursor-cell-enriched genes with the SOX2-enriched genes generated by Bracko et al. (2012) revealed only three common genes (*Igf1*, *Dab2*, and *Txnip*), and when our threshold was decreased to 2-fold enrichment only two additional commonly expressed genes were detected (*Ucp2* and *Hmgb2*). The fact that SOX2 also marks post-mitotic astrocytes and the presence of known choroid plexus markers in their stem cell gene list highlights the limitation of sorting using a single marker. In contrast, our division of proliferative versus non-proliferative corresponds well with subpopulations identified by transcript functional profiling in another recent study (Shin et al., 2015). Our present study extends on this work by enabling prospective isolation of the proliferative and non-proliferative precursor cell populations. This will allow downstream manipulation in vitro for further characterization of factors capable of activating the quiescent stem cells, as well as for potential applications such as transplantation.

Transcriptomic analysis of our isolated proliferative precursor population revealed a profile with immune-like characteristics. The presence of cytokine receptors on neural precursor cells, as well as the production of cytokines and other inflammatory molecules, supports the existence of bidirectional crosstalk between the neural stem cells and the immune system (Zhang et al., 2015). Indeed, there is emerging evidence for a direct and synergistic interaction between neural stem cells and peripheral T cells to maintain baseline neurogenesis levels as well as to promote recovery following insult (Niebling et al., 2014; Wolf et al., 2009; Zhang et al., 2015). Our analysis revealed a number of immune molecules expressed by the proliferative precursor cells, most of which have no known role in the regulation of adult neural stem cells. We had, however, previously identified one of these molecules, Oncostatin M, as a regulator of neural precursor activity (Beatus et al., 2011). In addition, as a proof of concept, we confirmed a regulatory role of one of the identified immune-related proteins in adult hippocampal precursor proliferation. More detailed studies, however, are required to further investigate the specific role that CXCL1 and the other stem-cell-specific cytokines play in this process.

The definition of marker combinations in neural stem cell biology has been hampered by the dearth of information linking markers and the underlying lineage-defining biology. LPA is of particular interest as it suggests lipids as a new class of molecules co-defining stem cell entities, and indeed lipids are emerging as key signaling molecules in neural stem cell biology. The most abundant brain lipid, DHA (docosahexaenoic acid), is consistently released from phospholipids, and its presence is inversely linked to brain aging and neurodegenerative diseases. DHA supplementation leads to enhanced hippocampal long-term potentiation (Kawashima et al., 2010) and, combined with physical activity, enhances synaptic plasticity and spatial learning (Wu et al., 2008). DHA increases neurogenesis in vitro and in vivo (Kawakita et al., 2006). Another dietary polyunsaturated fatty acid, arachidonic acid, has also been shown to enhance hippocampal neurogenesis (Maekawa et al., 2009). We show that exogenous LPA affects in vitro precursor cell potential as well as proliferative capacity. This is in contrast to a previous report of reduced neurosphere size from LPA-treated cortical cells (Fukushima et al., 2007). Neurosphere numbers were not quantified in that study. Another study, using 10 μM LPA, showed inhibition of neurosphere formation and neuronal differentiation of human embryonic stem cells without affecting proliferation, apoptosis, or astrocytic differentiation (Dottori et al., 2008). Conversely, in embryonic brain cultures ex vivo, LPA promoted survival and differentiation of cortical precursor cells (Kingsbury et al., 2003). We found a significant stimulatory effect of LPA on adult hippocampal neurogenesis in vivo. Interestingly, only a small and statistically non-significant increase in proliferating precursor cell number in the LPA-infused group was seen. This is consistent with data showing that LPA can promote differentiation and cell survival without eliciting a strong proliferative response (Tang et al., 2014). Lipids have a critical role in cell signaling, with LPA binding G-protein-coupled receptors of the LPA receptor family (LPA_{1-6}) which signal via the PI3K-AKT, Ras-ERK, and PLC-PKC cell-signaling pathways. Cell survival is largely mediated by AKT signaling whereas the MAPK pathway generally regulates differentiation and cell specification, and the Rho and PKC pathways mediate proliferation (Gude et al., 2006; Miyamoto et al., 2009; Ye et al., 2002). Our present data showing an activation of AKT and MAPK pathway signaling explains the pro-survival effect observed in response to exogenous LPA. However, the exact mechanism through which LPA_1 activation is involved in the control of precursor cell activity and adult neurogenesis remains to be explored.

In summary, we show that LPA_1 is expressed by a defined population of neural precursor cells in the hippocampus, and provide evidence for the involvement of LPA in the regulation of these cells both in vitro and in vivo. In addition, we present a marker combination that allows the separation of proliferative and non-proliferative precursor cells and present the transcriptional profile of the proliferative cells, providing insight into their immune-like characteristics and further supporting the hypothesis of a bidirectional crosstalk between neural stem cells and the immune system.

EXPERIMENTAL PROCEDURES

For a more detailed description, see Supplemental Experimental Procedures.

Animals

LPA_1-GFP (Gong et al., 2003), Nestin-GFP (Yamaguchi et al., 2000), and Nestin-Cyan nuclear (Encinas and Enikolopov, 2008) mice were maintained on a 12-/12-hr light/dark cycle with food and water provided ad libitum. All experiments were conducted in accordance with the applicable European and national regulations (Tierschutzgesetz) and were approved by the responsible authority (Landesdirektion Sachsen). All animals were 8 weeks old at the time of the experiment except for the Nestin-Cyan/LPA_1-GFP mice, which were 3 weeks old.

Fluorescence Immunohistochemistry of Tissue Sections

Fluorescence immunohistochemistry was performed using the following primary antibodies: GFP, GFAP, vimentin, SOX2, TBR2, NeuN, calretinin, DCX, NeuroD, or S100β. The appropriate DyLight and cyanine secondary antibodies (1:500; Dianova) were used. For visualization of the blood vessels, biotinylated *Lycopersicon esculentum* (tomato lectin; 1:2,000; Vector Laboratories, Linaris) was added for 48 hr at 4°C, followed by incubation with streptavidin-Cy3 (1:500; Jackson ImmunoResearch Laboratories) and DAPI (1:10,000; Invitrogen). Fluorescence immunohistochemistry for the detection of CldU, IdU, and NeuN was performed as described previously (Overall et al., 2013).

Fluorescence-Activated Cell Sorting and In Vitro Cell Culture

Dentate gyrus tissue from Nestin-GFP or LPA_1-GFP mice (eight per experiment) was microdissected (Hagihara et al., 2009) and enzymatically dissociated using the Neural Tissue Dissociation Kit (Miltenyi). Cells were stained with a prominin-1-specific antibody (13A4-phycoerythrin [PE]; eBioscience) and/or EGF-647 (Molecular Probes). Prior to adding the prominin-1-PE or EGF-647, a small proportion of the cells were removed and stained with an isotype control (rat IgG1-PE; eBioscience) as a control for non-specific staining. Dead cells were excluded by staining with propidium iodide (1 μg/ml). Sorted populations of cells were collected directly into neurosphere growth medium, and each population was plated into 48 wells of a 96-well plate as described elsewhere (Walker and Kempermann, 2014). Primary hippocampal neurospheres were passaged from wells containing single large neurospheres. For differentiation, neurospheres were plated onto poly-D-lysine (PDL) and laminin-coated coverslips in medium without growth factors for 8 days. The primary cells from each sorted population were plated into one well of a PDL/laminin-coated 24-well plate in 1 ml of growth medium to generate adherent monolayer cultures. The cells were stained for βIII-tubulin, MAP2ab, GFAP, the oligodendrocyte marker O4, or the precursor cell antigen Nestin.

For the in vitro neurosphere experiments, primary dentate gyrus cells were isolated and either LPA (18:1 1-oleoyl-2-hydroxy-sn-glycero-3-phosphate, 10 μM; Avanti Polar Lipids), DGPP (8:0 dioctanoylglycerol pyrophosphate, 50 μM; Avanti Polar Lipids), KCl (15 mM), CXCL1 (3 ng/ml or 30 ng/ml; R&D Systems), CXCL2 (0.1 ng/ml, 1 ng/ml, or 10 ng/ml; R&D Systems), or CCL8 (10 ng/ml or 100 ng/ml; BioLegend) were added at the time of plating.

BrdU and GFP Immunohistochemistry and Quantification

For assessment of cell proliferation in the dentate gyrus, LPA_1-GFP mice were given three intraperitoneal injections of 50 mg/kg BrdU (Sigma) spaced 6 hr apart, and were perfused 12 hr after the last injection.

For quantification of $BrdU^+$ and GFP^+ cells in the dentate gyrus, sections were stained for either BrdU or GFP, followed by incubation with anti-rat-biotin or anti-rabbit-biotin secondary antibodies (both 1:500; Dianova). Detection was performed using the Vectastain ABC-Elite reagent (Vector Labs, Linaris) with diaminobenzidine (Sigma) and 0.04% NiCl as the chromogen.

Next-Generation Sequencing

Three populations of primary dentate gyrus cells, "proliferative LPA_1^+ cells" (LPA_1-GFP^+EGFR^+prominin-1^+), "non-proliferative LPA_1^+ cells" (LPA_1-GFP^+EGFR^+prominin-1^-, LPA_1-GFP^+EGF^-prominin-1^+, and LPA_1-GFP^+EGFR^-prominin-1^-), and "niche cells" (LPA_1-GFP^-), were isolated by FACS and pools of approximately 1,000 cells were sequenced on the Illumina HiSeq 2000 platform providing on average 35 Mio reads per sample. The raw sequence data are deposited in the GEO under accession number GEO: GSE68270. Reads were mapped to the latest mouse genome build (mm10) and counts per gene were $\log_2$-transformed for downstream analysis. Population-specific transcripts were identified by first using an ANOVA filter (adjusted $p < 0.05$) and then selecting transcripts with more than 4-fold difference in expression between groups. Comparison with single-cell data (Shin et al., 2015) employed an eigengene derived from transcripts corresponding to the genes differentially regulated in this study (Table S1).

In Vivo LPA Infusion

Micro-osmotic pumps (Alzet, #1004; 28 days of infusion at a flow rate of 0.11 μl/hr) were loaded with LPA (200 nM) supplemented with 0.1% BSA or vehicle solution (0.9% sterile PBS, containing 0.1% BSA), and the cannula inserted to enable unilateral infusion directly into the hilus region of the hippocampus (anterior/posterior −1.3, dorsal/lateral +1.0, dorsal/ventral −2.2, relative to

Bregma). Mice were injected with CldU (42.5 mg/kg) immediately following surgery on day 1 and with IdU (57.5 mg/kg) on the evening of the 28th day, 12 hr prior to perfusion.

Protein Preparation and Western Blot Analysis

LPA_1-GFP$^+$ adherent cultures were transferred to mitogen-free medium for 24 hr, after which LPA (25 μM) was added and the cells were incubated for 2, 5, 10, 30, or 60 min at 37°C. For the ex vivo experiments primary dentate gyrus cells were isolated and treated with either PBS or LPA (25 μM) for 10 min in either the presence or absence of the LPA_1-specific inhibitor DGPP (50 μM). They were then lysed immediately on ice and clarified by centrifugation at 16,000 × *g* for 10 min at 4°C. Lysates were separated on 4%–12% NuPage gels and transferred to polyvinylidene fluoride membranes, and probed with either rabbit anti-AKT, rabbit anti-phospho AKT-S473, or mouse anti-phospho ERK1/2 antibodies. Immunoreactive bands were detected using either donkey anti-rabbit horseradish peroxidase or goat anti-mouse secondary antibodies and the Super-Signal West Dura Chemiluminescent Substrate (Thermo Scientific).

ACCESSION NUMBERS

The accession number for the next generation sequence data reported in this paper is GEO: GSE68270.

SUPPLEMENTAL INFORMATION

Supplemental Information includes Supplemental Experimental Procedures, five figures, and four tables and can be found with this article online at http://dx.doi.org/10.1016/j.stemcr.2016.03.002.

AUTHOR CONTRIBUTIONS

T.L.W., K.F., and G.K. designed the study. T.L.W., A.M.S., S.V., D.L., S.R., M.I., and K.F. performed the experiments. T.L.W. and R.W.O. analyzed the data. T.L.W., R.W.O., K.F., and G.K. wrote the manuscript.

ACKNOWLEDGMENTS

T.L.W. was supported by a Marie Curie International Incoming Fellowship. This work was partly funded by Deutsche Forschungsgemeinschaft SFB 655. The project was otherwise financed from basic institutional funding. We thank Anne Karasinsky for care and maintenance of animals, Katja Schneider and Nicole Rund for assistance with FACS, Masuhiro Yamaguchi for providing the Nestin-GFP mice, Grigori Enikolopov for providing Nestin-Cyan nuclear mice, Ronald Naumann for the in vitro fertilization to generate the LPA_1-GFP mice, Silke White for microscopy assistance, Maciej Paszkowski-Rogacz for making his fpkem software available, and Andreas Dahl, Sylvia Klemroth, and Annekathrin Kränkel from the Deep Sequencing Group SFB 655 for technical support in performing the RNA-sequencing experiments.

Received: December 17, 2015
Revised: March 3, 2016
Accepted: March 3, 2016
Published: March 31, 2016

REFERENCES

Beatus, P., Jhaveri, D.J., Walker, T.L., Lucas, P.G., Rietze, R.L., Cooper, H.M., Morikawa, Y., and Bartlett, P.F. (2011). Oncostatin M regulates neural precursor activity in the adult brain. Dev. Neurobiol. *71*, 619–633.

Beech, R.D., Cleary, M.A., Treloar, H.B., Eisch, A.J., Harrist, A.V., Zhong, W., Greer, C.A., Duman, R.S., and Picciotto, M.R. (2004). Nestin promoter/enhancer directs transgene expression to precursors of adult generated periglomerular neurons. J. Comp. Neurol. *475*, 128–141.

Bracko, O., Singer, T., Aigner, S., Knobloch, M., Winner, B., Ray, J., Clemenson, G.D., Jr., Suh, H., Couillard-Despres, S., Aigner, L., et al. (2012). Gene expression profiling of neural stem cells and their neuronal progeny reveals IGF2 as a regulator of adult hippocampal neurogenesis. J. Neurosci. *32*, 3376–3387.

Castilla-Ortega, E., Hoyo-Becerra, C., Pedraza, C., Chun, J., Rodriguez De Fonseca, F., Estivill-Torrus, G., and Santin, L.J. (2011). Aggravation of chronic stress effects on hippocampal neurogenesis and spatial memory in LPA(1) receptor knockout mice. PLoS One *6*, e25522.

Choi, J.W., Herr, D.R., Noguchi, K., Yung, Y.C., Lee, C.W., Mutoh, T., Lin, M.E., Teo, S.T., Park, K.E., Mosley, A.N., et al. (2010). LPA receptors: subtypes and biological actions. Annu. Rev. Pharmacol. Toxicol. *50*, 157–186.

Codega, P., Silva-Vargas, V., Paul, A., Maldonado-Soto, A.R., Deleo, A.M., Pastrana, E., and Doetsch, F. (2014). Prospective identification and purification of quiescent adult neural stem cells from their in vivo niche. Neuron *82*, 545–559.

Couillard-Despres, S., Winner, B., Karl, C., Lindemann, G., Schmid, P., Aigner, R., Laemke, J., Bogdahn, U., Winkler, J., Bischofberger, J., et al. (2006). Targeted transgene expression in neuronal precursors: watching young neurons in the old brain. Eur. J. Neurosci. *24*, 1535–1545.

Dottori, M., Leung, J., Turnley, A.M., and Pebay, A. (2008). Lysophosphatidic acid inhibits neuronal differentiation of neural stem/progenitor cells derived from human embryonic stem cells. Stem Cells *26*, 1146–1154.

Encinas, J.M., and Enikolopov, G. (2008). Identifying and quantitating neural stem and progenitor cells in the adult brain. Methods Cell Biol. *85*, 243–272.

Estivill-Torrus, G., Llebrez-Zayas, P., Matas-Rico, E., Santin, L., Pedraza, C., De Diego, I., Del Arco, I., Fernandez-Llebrez, P., Chun, J., and De Fonseca, F.R. (2008). Absence of LPA1 signaling results in defective cortical development. Cereb. Cortex *18*, 938–950.

Franceschini, A., Szklarczyk, D., Frankild, S., Kuhn, M., Simonovic, M., Roth, A., Lin, J., Minguez, P., Bork, P., von Mering, C., et al. (2013). STRING v9.1: protein-protein interaction networks, with increased coverage and integration. Nucleic Acids Res. *41*, D808–D815.

Fukushima, N., Shano, S., Moriyama, R., and Chun, J. (2007). Lysophosphatidic acid stimulates neuronal differentiation of cortical neuroblasts through the LPA1-G(i/o) pathway. Neurochem. Int. *50*, 302–307.

Gong, S., Zheng, C., Doughty, M.L., Losos, K., Didkovsky, N., Schambra, U.B., Nowak, N.J., Joyner, A., Leblanc, G., Hatten,

M.E., et al. (2003). A gene expression atlas of the central nervous system based on bacterial artificial chromosomes. Nature *425*, 917–925.

Gude, N., Muraski, J., Rubio, M., Kajstura, J., Schaefer, E., Anversa, P., and Sussman, M.A. (2006). Akt promotes increased cardiomyocyte cycling and expansion of the cardiac progenitor cell population. Circ. Res. *99*, 381–388.

Hagihara, H., Toyama, K., Yamasaki, N., and Miyakawa, T. (2009). Dissection of hippocampal dentate gyrus from adult mouse. J. Vis. Exp. http://dx.doi.org/10.3791/1543.

Heintz, N. (2004). Gene expression nervous system atlas (GENSAT). Nat. Neurosci. *7*, 483.

Hodge, R.D., Kowalczyk, T.D., Wolf, S.A., Encinas, J.M., Rippey, C., Enikolopov, G., Kempermann, G., and Hevner, R.F. (2008). Intermediate progenitors in adult hippocampal neurogenesis: Tbr2 expression and coordinate regulation of neuronal output. J. Neurosci. *28*, 3707–3717.

Jhaveri, D.J., Mackay, E.W., Hamlin, A.S., Marathe, S.V., Nandam, L.S., Vaidya, V.A., and Bartlett, P.F. (2010). Norepinephrine directly activates adult hippocampal precursors via beta3-adrenergic receptors. J. Neurosci. *30*, 2795–2806.

Kawaguchi, A., Miyata, T., Sawamoto, K., Takashita, N., Murayama, A., Akamatsu, W., Ogawa, M., Okabe, M., Tano, Y., Goldman, S.A., et al. (2001). Nestin-EGFP transgenic mice: visualization of the self-renewal and multipotency of CNS stem cells. Mol. Cell Neurosci. *17*, 259–273.

Kawakita, E., Hashimoto, M., and Shido, O. (2006). Docosahexaenoic acid promotes neurogenesis in vitro and in vivo. Neuroscience *139*, 991–997.

Kawashima, A., Harada, T., Kami, H., Yano, T., Imada, K., and Mizuguchi, K. (2010). Effects of eicosapentaenoic acid on synaptic plasticity, fatty acid profile and phosphoinositide 3-kinase signaling in rat hippocampus and differentiated PC12 cells. J. Nutr. Biochem. *21*, 268–277.

Kempermann, G., Jessberger, S., Steiner, B., and Kronenberg, G. (2004). Milestones of neuronal development in the adult hippocampus. Trends Neurosci. *27*, 447–452.

Kingsbury, M.A., Rehen, S.K., Contos, J.J., Higgins, C.M., and Chun, J. (2003). Non-proliferative effects of lysophosphatidic acid enhance cortical growth and folding. Nat. Neurosci. *6*, 1292–1299.

Knobloch, M., Braun, S.M., Zurkirchen, L., von Schoultz, C., Zamboni, N., Arauzo-Bravo, M.J., Kovacs, W.J., Karalay, O., Suter, U., Machado, R.A., et al. (2013). Metabolic control of adult neural stem cell activity by Fasn-dependent lipogenesis. Nature *493*, 226–230.

Maekawa, M., Takashima, N., Matsumata, M., Ikegami, S., Kontani, M., Hara, Y., Kawashima, H., Owada, Y., Kiso, Y., Yoshikawa, T., et al. (2009). Arachidonic acid drives postnatal neurogenesis and elicits a beneficial effect on prepulse inhibition, a biological trait of psychiatric illnesses. PLoS One *4*, e5085.

Matas-Rico, E., Garcia-Diaz, B., Llebrez-Zayas, P., Lopez-Barroso, D., Santin, L., Pedraza, C., Smith-Fernandez, A., Fernandez-Llebrez, P., Tellez, T., Redondo, M., et al. (2008). Deletion of lysophosphatidic acid receptor LPA1 reduces neurogenesis in the mouse dentate gyrus. Mol. Cell Neurosci. *39*, 342–355.

Mignone, J.L., Kukekov, V., Chiang, A.S., Steindler, D., and Enikolopov, G. (2004). Neural stem and progenitor cells in nestin-GFP transgenic mice. J. Comp. Neurol. *469*, 311–324.

Miyamoto, S., Murphy, A.N., and Brown, J.H. (2009). Akt mediated mitochondrial protection in the heart: metabolic and survival pathways to the rescue. J. Bioenerg. Biomembr. *41*, 169–180.

Niebling, J., E Rünker, A., Schallenberg, S., Kretschmer, K., and Kempermann, G. (2014). Myelin-specific T helper 17 cells promote adult hippocampal neurogenesis through indirect mechanisms. F1000Res. *3*, 169.

Overall, R.W., Walker, T.L., Leiter, O., Lenke, S., Ruhwald, S., and Kempermann, G. (2013). Delayed and transient increase of adult hippocampal neurogenesis by physical exercise in DBA/2 mice. PLoS One *8*, e83797.

Pastrana, E., Cheng, L.C., and Doetsch, F. (2009). Simultaneous prospective purification of adult subventricular zone neural stem cells and their progeny. Proc. Natl. Acad. Sci. USA *106*, 6387–6392.

Santin, L.J., Bilbao, A., Pedraza, C., Matas-Rico, E., Lopez-Barroso, D., Castilla-Ortega, E., Sanchez-Lopez, J., Riquelme, R., Varela-Nieto, I., de la Villa, P., et al. (2009). Behavioral phenotype of maLPA1-null mice: increased anxiety-like behavior and spatial memory deficits. Genes Brain Behav. *8*, 772–784.

Shin, J., Berg, D.A., Zhu, Y., Shin, J.Y., Song, J., Bonaguidi, M.A., Enikolopov, G., Nauen, D.W., Christian, K.M., Ming, G.L., et al. (2015). Single-cell RNA-Seq with waterfall reveals molecular cascades underlying adult neurogenesis. Cell Stem Cell *17*, 360–372.

Suh, H., Consiglio, A., Ray, J., Sawai, T., D'Amour, K.A., and Gage, F.H. (2007). In vivo fate analysis reveals the multipotent and self-renewal capacities of Sox2+ neural stem cells in the adult hippocampus. Cell Stem Cell *1*, 515–528.

Tang, N., Zhao, Y., Feng, R., Liu, Y., Wang, S., Wei, W., Ding, Q., An, M.S., Wen, J., and Li, L. (2014). Lysophosphatidic acid accelerates lung fibrosis by inducing differentiation of mesenchymal stem cells into myofibroblasts. J. Cell Mol. Med. *18*, 156–169.

van Praag, H., Kempermann, G., and Gage, F.H. (1999). Running increases cell proliferation and neurogenesis in the adult mouse dentate gyrus. Nat. Neurosci. *2*, 266–270.

Walker, T.L., and Kempermann, G. (2014). One mouse, two cultures: isolation and culture of adult neural stem cells from the two neurogenic zones of individual mice. J. Vis. Exp. e51225.

Walker, T.L., Yasuda, T., Adams, D.J., and Bartlett, P.F. (2007). The doublecortin-expressing population in the developing and adult brain contains multipotential precursors in addition to neuronal-lineage cells. J. Neurosci. *27*, 3734–3742.

Walker, T.L., White, A., Black, D.M., Wallace, R.H., Sah, P., and Bartlett, P.F. (2008). Latent stem and progenitor cells in the hippocampus are activated by neural excitation. J. Neurosci. *28*, 5240–5247.

Walker, T.L., Wierick, A., Sykes, A.M., Waldau, B., Corbeil, D., Carmeliet, P., and Kempermann, G. (2013). Prominin-1 allows prospective isolation of neural stem cells from the adult murine hippocampus. J. Neurosci. *33*, 3010–3024.

Wolf, S.A., Steiner, B., Akpinarli, A., Kammertoens, T., Nassenstein, C., Braun, A., Blankenstein, T., and Kempermann, G. (2009). CD4-positive T lymphocytes provide a neuroimmunological link in the

control of adult hippocampal neurogenesis. J. Immunol. *182*, 3979–3984.

Wu, A., Ying, Z., and Gomez-Pinilla, F. (2008). Docosahexaenoic acid dietary supplementation enhances the effects of exercise on synaptic plasticity and cognition. Neuroscience *155*, 751–759.

Yamaguchi, M., Saito, H., Suzuki, M., and Mori, K. (2000). Visualization of neurogenesis in the central nervous system using nestin promoter-GFP transgenic mice. Neuroreport *11*, 1991–1996.

Ye, X., Fukushima, N., Kingsbury, M.A., and Chun, J. (2002). Lysophosphatidic acid in neural signaling. Neuroreport *13*, 2169–2175.

Zhang, H., Shao, B., Zhuge, Q., Wang, P., Zheng, C., Huang, W., Yang, C., Wang, B., Su, D.M., and Jin, K. (2015). Cross-talk between human neural stem/progenitor cells and peripheral blood mononuclear cells in an allogeneic co-culture model. PLoS One *10*, e0117432.